

Developing Low-Amplitude Pulsating Laminar Flow In A Flat Channel

Purdin Michail Sergeevich

National Research University "Moscow Power Engineering Institute", Moscow, Russia.

ORCID: 0000-0002-5601-4845

Abstract

A mathematical model and a method of numerical modeling of a developing low-amplitude pulsating laminar flow in a flat channel based on the boundary layer theory was developed. Hydrodynamic characteristics of laminar flows pulsating with low amplitudes at the entrance hydrodynamic length are presented and analyzed.

Keywords: hydrodynamics, flat channel, pulsating flow, laminar flow, entrance hydrodynamic length.

I. INTRODUCTION

Recently, there has been a significant amount of interest in the application of microchannel reaction apparatus [1]. Due to their high compactness, a high intensity of heat and mass transfer and a high rate of diffusion and chemical processes can be achieved. As a result, there is a high degree of completion of a chemical reaction. Therefore, there is an opportunity to use for its realization energy resources (including secondary resources) with a lower temperature level. Due to the small size of the microchannels of such devices, the Reynolds number Re does not exceed 2000. That is a reason why the flow regime in such channels is laminar. Heat exchangers with rectangular channels are more frequently used for cooling electronic equipment.

In the field of biology, it is important to know the mechanism of the laminar pulsating flow while modeling the human breathing, the movement of blood in arteries and capillaries. In some cases, such flow is also carried out in biological microchip systems, which have a high development level last years (see, for example, [2]). These systems are designed to diagnose the activity of various human's organs as well as for targeted and precisely dosed delivery of medicaments to them. Pneumatic micropumps with periodic displacement of fluid from free volumes are used for biomedical researches. Thus, a realization of calculating researches in this scientific field is important from practical and theoretical points of view.

The entrance hydrodynamic length, defined as the distance from the channel entrance, where the velocity on the axis is 99% of the velocity on the axis for a fully developed flow ($U_{Y=0} = 0,99U_{Y=0, X \rightarrow \infty}$), for a laminar pulsating flow in accordance with the information [3] with the flow rate pulsating having relatively small frequency remains the same as with a steady flow.

At present, there is insufficient information about the effect of pulsations of the laminar flow on the entrance hydrodynamic length and on the changing of hydrodynamic values along a channel length, which are necessary for a hydraulic calculation of microchannel biochips and heat exchangers.

II. PROBLEM DEFINITION AND VALIDATION

The distribution of the velocity components for a developing low-amplitude pulsating laminar flow in a flat channel is described by the following motion equation:

$$\frac{\partial u}{\partial t} + u \frac{\partial u}{\partial x} + v \frac{\partial u}{\partial y} = \nu \frac{\partial^2 u}{\partial y^2} - \frac{1}{\rho} \frac{dp}{dx} \quad (1)$$

and the following continuity equation:

$$\frac{\partial u}{\partial x} + \frac{\partial v}{\partial y} = 0, \quad (2)$$

where p is the pressure, t is the time, u and v are the velocities correspondingly along the x and y axis, ν is the kinematic viscosity, ρ is the density.

This form of equations (1) and (2) corresponds to the boundary layer theory, and it is obtained by neglecting the terms in the full system of Navier–Stokes equations with a small order of value [4]. Since $v \ll u$, there is no necessity in solving the equation of the momentum conservation law for the transverse velocity component. This kind of simplification was applied to solve the issue of a developing steady flow analytically in [5] and later numerically in [6]. The transverse velocity component has some influence both on solving the heat or mass transfer equation and on solving the motion equation (1). When $Re < 100$, it is impossible to neglect the solution of the motion equation for the transverse velocity component, since the entrance length becomes comparable or smaller than the height of the channel, and the transverse velocity component becomes comparable or larger than the longitudinal velocity component. The research area is limited by the Reynolds number in the range of $100 < Re < 2000$.

There are equations (1) and (2) for velocity, which have to be supplemented with an equation for finding the pressure gradient. This equation is obtained based on the integral continuity equation and is presented in the method of numerical solution.

In a dimensionless form for a pulsating flow equations (1), (2) have the following form:

$$S^2 \frac{\partial U}{\partial t_\omega} + U \frac{\partial U}{\partial X} + V \frac{\partial U}{\partial Y} = \frac{\partial^2 U}{\partial Y^2} + P, \quad (4)$$

$$\frac{\partial U}{\partial X} + \frac{\partial V}{\partial Y} = 0, \quad (5)$$

where $P = -\frac{d_h Re}{\rho < \bar{u} > dx} \frac{dp}{dx}$ is the dimensionless pressure gradient,

$Re = \frac{\langle \bar{u} \rangle d_h}{\nu}$ is the Reynolds number, $d_h = 2h$ is the hydraulic diameter, h is the channel height, $S = d_h \sqrt{\frac{\omega}{\nu}}$ is dimensionless pulsating frequency, $t_\omega = \omega t$ is the dimensionless time, $U = \frac{u}{\langle \bar{u} \rangle}$ and $V = \frac{v}{\langle \bar{u} \rangle}$ are the dimensionless longitudinal and transverse velocities, $X = \frac{x}{d_h}$ and $Y = \frac{y}{d_h}$ are the dimensionless longitudinal and transverse coordinates, ω is the rotational frequency, the signs $\langle \rangle$ and $\bar{}$ mean averaging over the cross section and over the time.

In practice, there is a pre-included space before entering of the channel. Since $A > 1$, the flow moves in the opposite direction during the part of the period and enters in this pre-included space, what is actually a problem for modeling a pulsating flow associated with a large number of its geometrical parameters. Since $A > 1 \wedge A \approx 1$, at some moments the transverse velocity component becomes comparable or larger than the longitudinal velocity component. In addition, for $A \approx 1$ secondary pulsations can occur, as two countercurrent flows occur in the pre-included space, what can lead to instability about the axis of symmetry and the formation of vortices. For these cases, the model has to be supplemented by the motion equation for the transverse velocity component. The considered model leaves out of account the pre-included space and the possible asymmetry of the flow, therefore, the amplitude of average velocity pulsations over the cross section is limited by the range $0 < A \ll 1$.

A computational domain scheme with boundary conditions is presented on the fig. 1. At the entrance to the channel (when $X = 0$) a uniform velocity profile is defined. This simplification is valid for the Reynolds number $Re > 100$, when the thickness of the dynamic boundary layer is small in comparison with the height of the channel. When $Y = Y_0$, the no-slip boundary condition is defined (the transverse and longitudinal velocities are equal to zero). When $Y = 0$, the symmetry condition is defined (the first derivative with respect to the transverse coordinate of the longitudinal velocity is zero and, accordingly, the transverse velocity is zero). At the output boundary (when $X = X_0$) the condition of flow stabilization is defined (the first derivative with respect to the longitudinal coordinate of the longitudinal velocity is zero and, accordingly, the transverse velocity is zero). The condition of flow stabilization is defined on distance X_0 which does not affect at the results of the calculations.

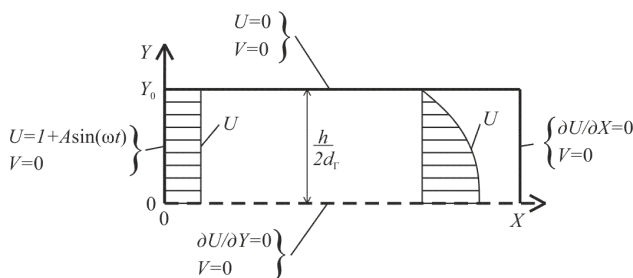


Fig. 1. Computational domain scheme.

The area of dimensionless pulsating frequencies is limited by $S > 0$.

III. METHODS OF NUMERICAL SOLUTION

The solution of the equation (4) was found by applying the finite difference method using an implicit stable time two-layer difference scheme. For approximation of the first derivative of the longitudinal coordinate, a “counter flow” scheme was used, since even for $A < 1$ with $S \gg 1$, reversal flows can occur close to the wall [7]. At the problem statement level, the research area is limited by regimes without reversal flows, but there is no information about whether they will occur when a developing pulsating flow takes place. A central difference scheme is applied for approximation of the first derivative of the transverse coordinate. It was done to increase the approximation order of accuracy along the transverse coordinate till the second level using a simpler scheme.

The given scheme is similar to the scheme for a steady developing flow, proposed and described in [8]. For the case of a pulsating flow only the non-stationary term was added to the motion equation and approximated with the first order.

The spatial grid used to solve the system of linear equations obtained from (4) and (5) is presented on the fig. 2. An equal partition along the longitudinal and transverse coordinates is applied. The number of partitions along the X , Y , t_ω coordinates was equal to $64 \times 64 \times 256$ and was found by successive doubling and by controlling of the difference of the obtaining results.

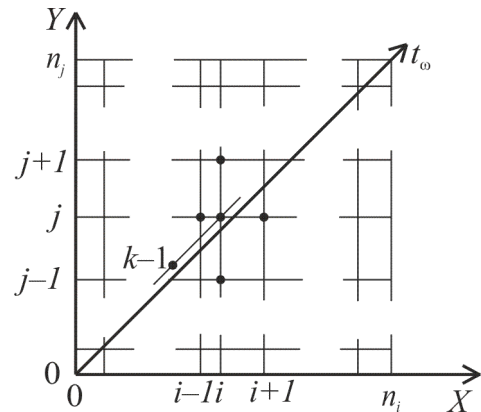


Fig. 2. Spatial grid.

To find the dimensionless pressure gradient P included in equation (4), the method was developed based on the fact the average velocity over the cross section is known at every moment of time.

$$P_{i,k}^n = P_{i,k}^{n-1} + P_s \frac{\langle U_k \rangle^* - \langle U_{i,k}^{n-1} \rangle}{|\langle U_{i,k}^{n-1} \rangle|}, \quad (9)$$

where P_s is the pressure gradient corresponding to a steady stabilized flow, $\langle U_k \rangle^* = 1 + A \sin(\omega t)$ is a given law of the average velocity changing over the cross section, n is the number of the pressure selection iteration. Since $\partial \langle U \rangle / \partial X = 0$ then there is $\langle U(X) \rangle = \langle U \rangle^* = 1 + A \sin(\omega t)$. During the iterations the certain value is added to P , that $\langle U(X) \rangle$ approaches $\langle U \rangle^*$. The equation (9) is a rule for selecting a pressure gradient so the integral continuity equation can be satisfied. It is evident that the right term in the equation becomes equal to

zero only when the average velocity over the cross section is equal to the given velocity. When the small pulsating amplitudes of A take place, the pressure gradient is close to its stationary value, therefore, the coefficient P_s is used to accelerate the convergence. As an initial approximation, the pressure gradient is defined like equal to P_s . This method of determining the pressure gradient allows to obtain its correct value including negative value, using small number of iterations, what is possible with pulsating flows with a high frequency.

The solution is carried out in the following order.

1. The system of linear equations for $U_{i,j,k}$, obtained from the equation (4) is solved with a checking of the setting of the velocity profile.
2. The values $P_{i,k}$ and $V_{i,j,k}$ are calculated.
3. The comparison of the pressure gradient change with the required accuracy should be done as well as the return to step 1. if there is a necessity.

To solve the systems of linear equations obtained from the equation (4), the Gauss-Seidel method was applied. It is well suited for multi-core computing devices, since it does not require a sequential transition from point to point, which is obligatory, for example, with the shuttle method. The ASUS STRIX R9 FURY video card was used for calculations as a high-performance coprocessor with a peak performance of 7.2 Tflop/s for single-precision numbers. The program [9] was created using the C++ language for the calculations where the C++AMP library was used to implement the calculations on the video card. A sufficient optimization of joint parallel calculations in the program between the central processor and the video card was carried out to increase the speed of its operation. The calculation time for one mode was less than 30 minutes.

The integration over the channel cross section was carried out by the Simpson method, and the integration over the time was made by the trapezoid method. The order of accuracy of this integration was highly competitive to the accuracy order of the

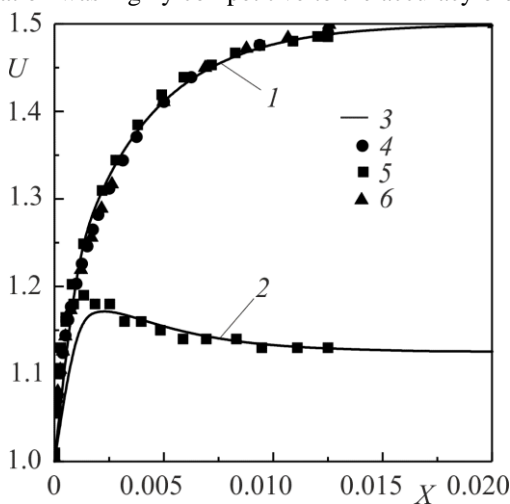


Fig. 3. Distribution of longitudinal velocity component along the channel length. 1 – for $Y = 0$, 2 – $0.5Y_0$; 3 – results of numerical solution, 4 – Boboia data [6], 5 – Sparrow data [11], 6 – Liu data [12].

difference approximation of differential equations, what allows to use machine resources efficiently.

IV. VERIFICATION OF HYDRODYNAMICS CALCULATIONS

Verification of the results of hydrodynamics calculations, obtained by using the program, was carried out before making the calculations in the given range of operating parameters. Up to the present moment, detailed researches of hydrodynamics with a pulsating flow at the entrance hydrodynamic length of a flat channel were not carried out. However, to verify the solution, it is possible to use the information about the steady developing flow and the stabilized pulsating flow.

The result of the calculation of the steady developing flow obtained by the presented method and the results of the calculations of other authors are presented on the fig. 3 and 4. To obtain this result the following input data were used in the program: $A = 0$, $S = 0$ and grid size is $64 \times 64 \times 1$.

The entrance hydrodynamic length (EHL), defined as the coordinate where the difference between the velocity in the center of the channel and the velocity in the center of the channel with a stabilized flow is 1%, was $L_{EHLs} = 0.0115$. The length of the closing of the boundary layers, which is determined analytically Targ S.M. [10], was $L = 0.00644$. It should be noted that the EHL was $L_{EHL} = 0.011$ in [11] and [12] and $L_{EHLs} = 0.0113$ in [13]. Thus, there is a sufficient accurate match of the results. It proves that the convective and diffusion terms in the motion equation are solved correctly as well as the method of finding the pressure gradient also works correctly.

Comparison of the velocity profile at different points of the time with a stabilized pulsating laminar flow obtained in the program [9] with the results of the calculation in the program [14] is presented on the fig. 5. The results of calculations in the program [14] were published in [7], [15], [16]. Velocity profiles are the same. It means that the chosen numerical scheme for approximating the nonstationary, convective (along the longitudinal coordinate) and diffusion term, as well as the developed method, work correctly.

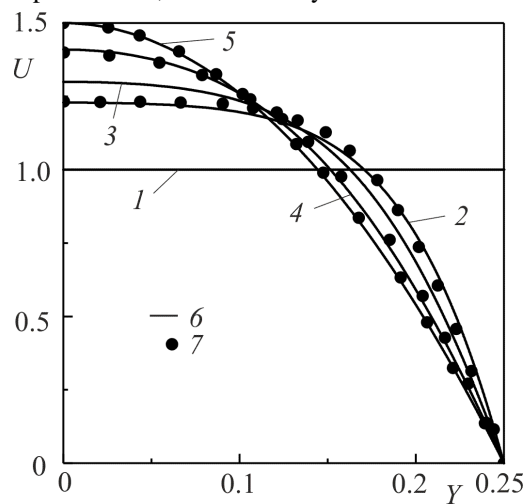


Fig. 4. Profiles of longitudinal velocity component. 1 – for $X = 0$, 2 – 0.001 , 3 – 0.002 , 4 – 0.005 , 5 – 0.0625 , 6 – results of numerical solution, 7 – Sparrow data [11].

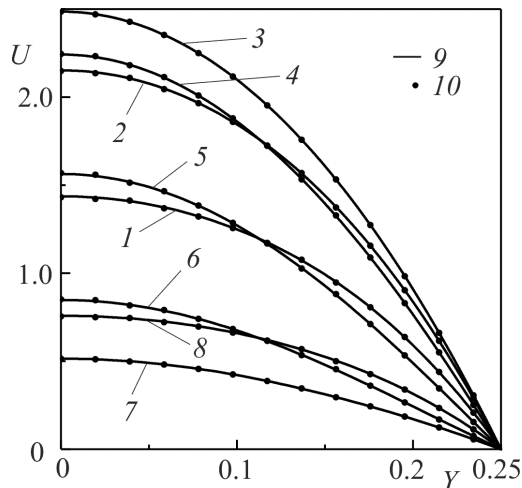


Fig. 5. Velocity profiles for $S = 8$ and $A = 2/3$. 1 – $t_\omega = 0$, 2 – $\pi/4$, 3 – $\pi/2$, 4 – $3\pi/4$, 5 – π , 6 – $5\pi/4$, 7 – $3\pi/2$, 8 – $7\pi/4$, 9 – results of numerical solution for $X = 0,0625$, 10 – data from program [14]

V. RESULTS

The change in the longitudinal velocity component on the channel axis is presented on the fig. 6a. It can be noticed that the time-averaged velocity \bar{U} coincides with the stationary U_S , regardless of the pulsating frequency S . The phase shift and the change in the amplitude of the velocity pulsating are distinctly noticeable while passing from the quasi-stationary to the high-frequency pulsating mode. The length of the hydrodynamic stabilization varies with time.

The changing in the coefficient of hydraulic resistance is presented on the fig. 6b. Time-averaged values of the pressure gradient \bar{P} correspond to the stationary P_S . The amplitude of pressure gradient pulsations increases with an increasing of the dimensionless pulsating frequency S .

Since $\bar{U} = U_S$, for convenience of analysis, the stationary velocity component is subtracted from the longitudinal velocity component and the pulsating velocity component $\tilde{U} = U - U_S$ is obtained. The pulsating component of the longitudinal velocity is average over the cross section $\langle \tilde{U} \rangle = A \sin(t\omega)$, then the point of strong interest is to consider the ratio \tilde{U}/A depending on the amplitude A and the pulsating frequency S of the average velocity over the cross section (see fig. 7).

With an increasing of the pulsating frequency (going from fig. 7a to 7b or from fig. 7c to 7d), looking at the changing of the profile's shape \tilde{U}/A at different points in time in a quasi-stationary mode ($S = 1$), the way how the profiles at every point of the channel cross section vary in accordance with the average over the cross section $\langle \tilde{U} \rangle$ and a shift in the phase of pulsating at $S = 8$ can be observed. Close to the entrance to the channel the phase displacement is almost negligible due to the fact that convective forces and the viscous friction prevail over the inertia, and further downstream the influence of the inertial

component increases relative to the others and reaches a maximum with a stabilized flow.

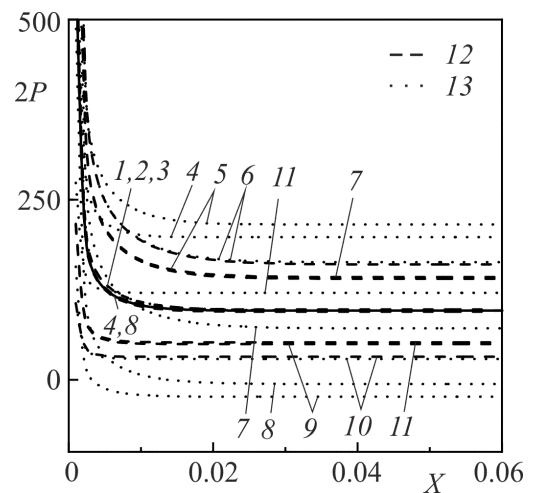
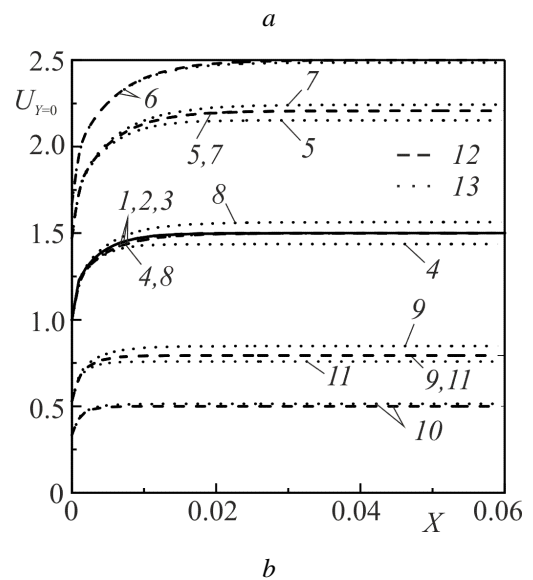


Fig. 6. Longitudinal velocity component at the channel axis (a) and the hydraulic drag coefficients (b) for $A = 2/3$. 1 – steady flow, 2 и 3 – average for $S = 1$ and $S = 8$; 4 – $t_\omega = 0$, 5 – $\pi/4$, 6 – $\pi/2$, 7 – $3\pi/4$, 8 – π , 9 – $5\pi/4$, 10 – $3\pi/2$, 11 – $7\pi/4$, 12 – $S = 1$, 13 – $S = 8$.

The appearance of a weak asymmetry of profile pulsating over the time can be observed with an increasing of average over the cross section pulsating amplitude of the velocity from $A = 1/3$ to $A = 2/3$ (going from fig. 7a to 7c or from fig. 7b to 7d). It proves the influence of the transverse velocity component, which becomes significant when the longitudinal velocity average over the cross section reaches its minimum value. When amplitudes of pulsating are $A < 2/3$, pulsations at the entrance hydrodynamic length over the whole cross section occur with the first harmonic of the frequency of average velocity pulsations over the cross section.

The pulsating component of the transverse velocity $\tilde{V} = V - V_S$ related to the amplitude of pulsations is presented on the fig. 8. Similar phenomena, as for the longitudinal velocity component, are observed, what is a consequence of the direct connection of these components through the continuity

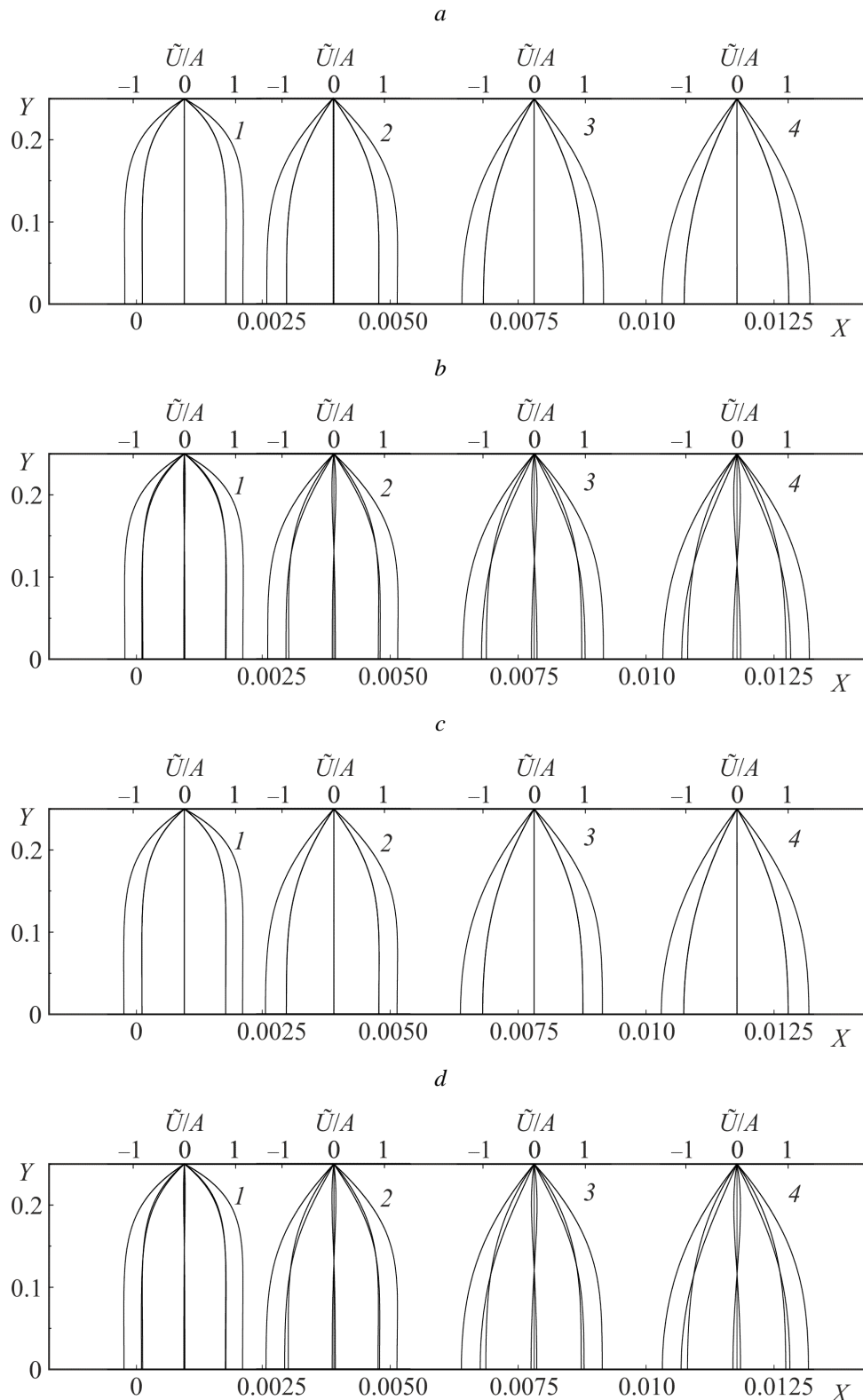


Fig. 7. Profiles of longitudinal pulsating velocity component for various time moment over the cross section $X = 0,001$ (1), $X = 0,004$ (2), $X = 0,008$ (3), $X = 0,012$ (4). *a* – for $A = 1/3$ and $S = 1$, *b* – $A = 1/3$ and $S = 8$, *c* – $A = 2/3$ and $S = 1$, *d* – $A = 2/3$ and $S = 8$.

equation. The motion equation is dominant in the system of equations (1) and (2). Equation (1) determines the physical laws for way how the flow will develop, since the influence of the transverse velocity on it is insignificant, what is confirmed by the results of the calculations.

Since for $A < 2/3$ the velocity pulsations at the entrance length of the channel occur according to a harmonic law, the calculation results can be presented as the distribution of the relative amplitude A_U/A and the pulsating phase φ_U of the pulsating velocity component (see fig. 9). It can be noticed that

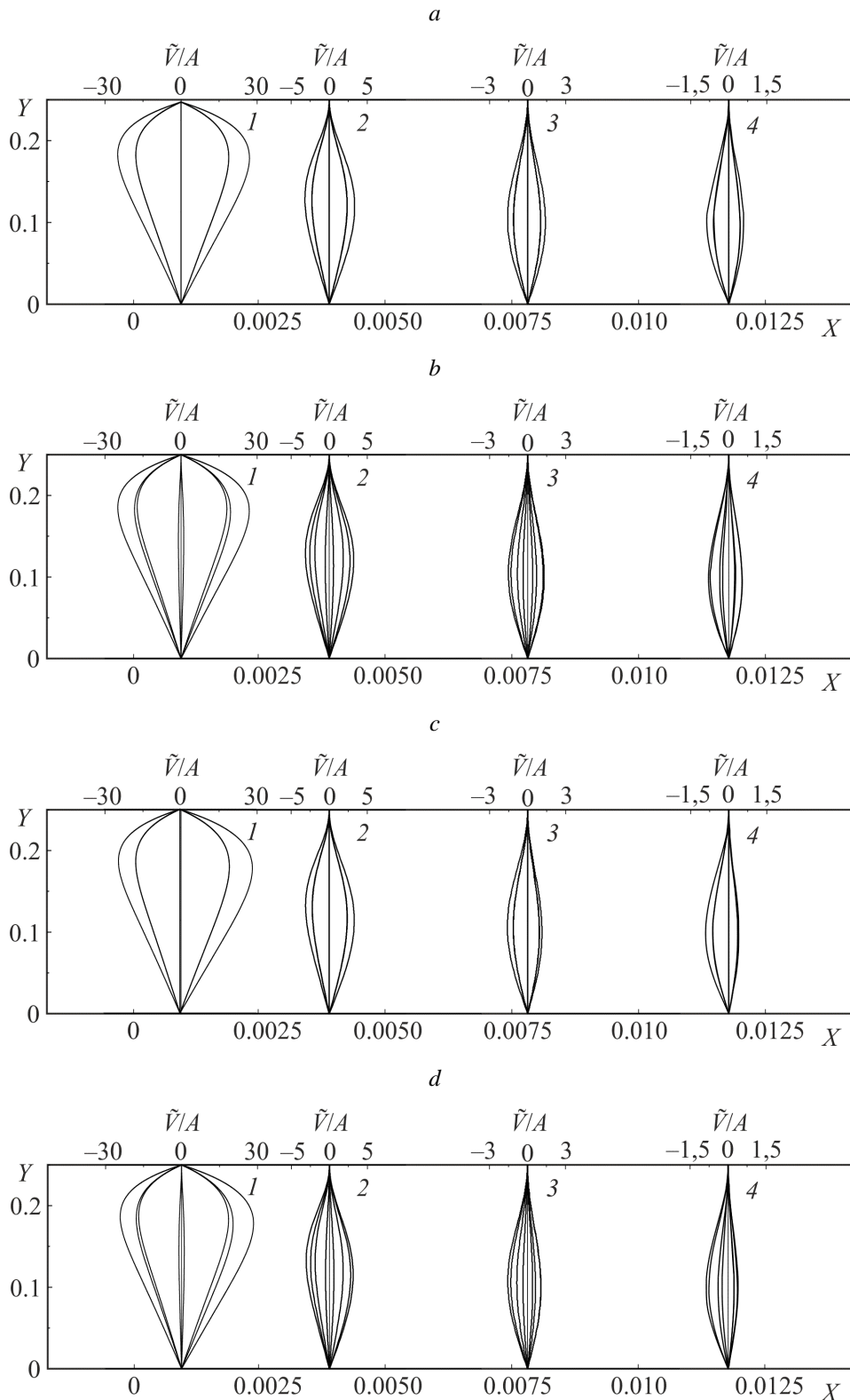


Fig. 8. Profiles of transverse pulsating velocity component for various time moment over the cross section $X = 0,001$ (1), $X = 0,004$ (2), $X = 0,008$ (3), $X = 0,012$ (4). *a* – for $A = 1/3$ and $S = 1$, *b* – $A = 1/3$ and $S = 8$, *c* – $A = 2/3$ and $S = 1$, *d* – $A = 2/3$ and $S = 8$.

in the low-frequency or in the quasi-stationary mode (see fig. 9a), the amplitude of pulsations on the axis monotonously increases along the channel length and decreases close to the wall. In the high-frequency mode of pulsations (see fig. 9b), the maximum amplitude of the pulsations shifts away from the

channel axis, and the distance, where the stabilization of the amplitude and the phase occurs, sharply decreases. The phase φ_U of pulsations close to the channel entrance is close to zero. Both in quasi-stationary (see fig. 9c) and in the high-frequency mode (see fig. 9d), it rearranges to the phase distribution for

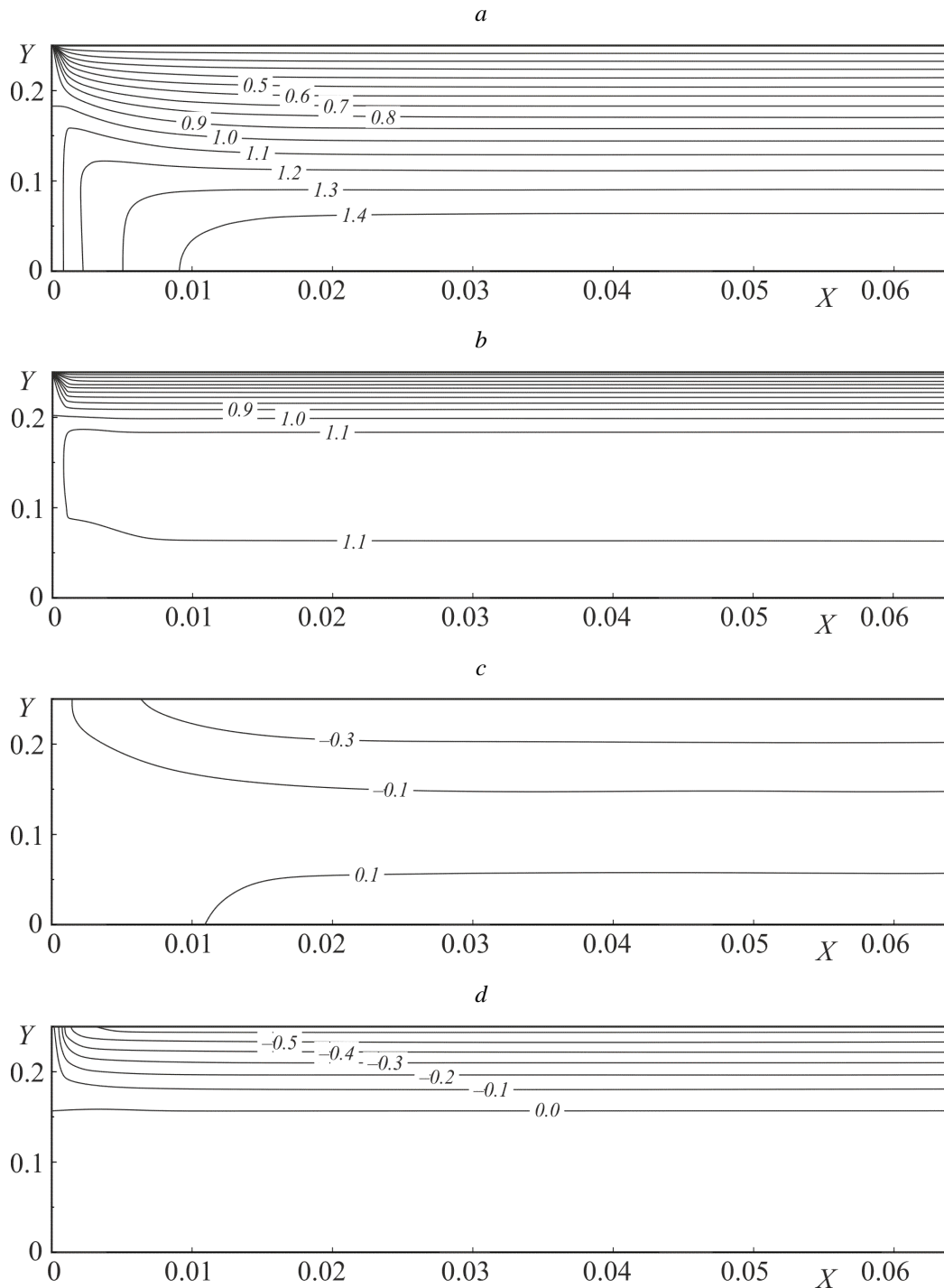


Fig. 9. Amplitude A_U/A (a, b) and phase φ_U (c, d) of the pulsations of longitudinal velocity component. a, c – $S = 4$; b, d – $S = 32$.

a stabilized pulsating flow monotonously along the channel.

The changing of the pulsation amplitude of the longitudinal velocity component A_U/A along the channel is presented on the fig. 10. It can be noticed that with an increasing of the pulsation frequency, the section length of its stabilization decreases, moreover, this section has the longest length on the channel axis.

The stabilization lengths of L_{EHL} , defined by $\bar{U}_{Y=0}(X)$, $(L_{EHL})_{max}$, defined as the maximum in the period, by $U_{Y=0}(X, t_\omega)$, $L_{AU/EHL}$ defined by the changing of A_U/A along

the channel length are presented on the fig. 11. The stabilization lengths along the channel were defined as the distance after which the magnitude changes no more than 1%. It follows from the obtained results that $L_{EHL} = L_{EHL,S}$ for any S and A . However, the maximum length of the entrance hydrodynamic length $(L_{EHL})_{max}$ is longer and increases with increasing the amplitude of pulsations. Since $S \rightarrow 0$ and amplitudes $A < 2/3$, the maximum length $(L_{EHL})_{max} \approx L_{EHL,S}(1 + A)$, and with increasing frequency it approaches $L_{EHL,S}$. In the quasi-stationary mode: $L_{AU/EHL} > L_{EHL,S}$. In the high-frequency mode ($S > 16$) $L_{AU/EHL}$ decreases sharply. Since a pulsating flow takes place, complete stabilization

during a period is achieved at slightly longer lengths than with a steady flow.

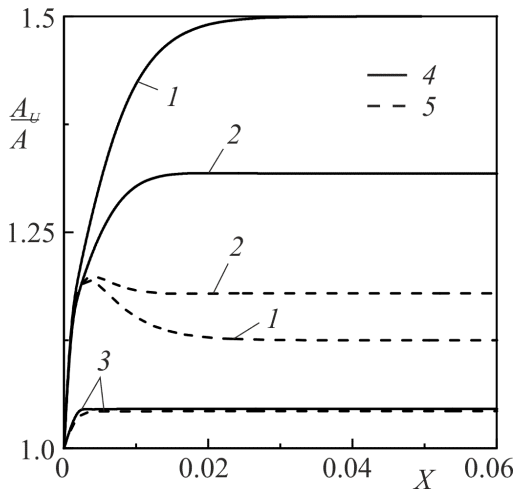


Fig. 10. Amplitude of the pulsations of longitudinal velocity component A_v/A . 1 – $S = 1$, 2 – $S = 16$, 3 – $S = 64$, 4 – $Y = 0$, 5 – $Y = 0,5Y_0$.

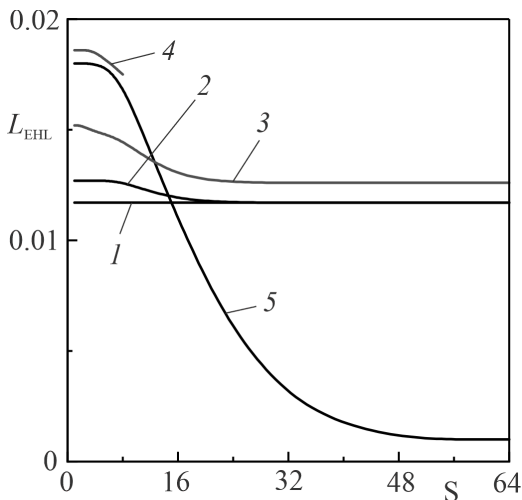


Fig. 11. The entrance hydraulic length $L_{EHL} - (1)$, $(L_{EHL})_{max} - (2, 3, 4)$, $L_{AUEHL} - (5)$. 2 – $A = 1/10$, 3 – $A = 1/3$, 4 – $A = 2/3$.

VI. CONCLUSION

A mathematical model and method of numerical simulation of a developing low-amplitude pulsating laminar flow in a flat channel based on the theory of the boundary layer was developed.

Time-averaged values of pressure gradient and velocity correspond to stationary values. The amplitude of pressure gradient pulsations increases with an increasing of the dimensionless pulsation frequency S .

Close to the entrance to the channel the displacement of the velocity pulsation phase is almost negligible due to the fact that convective forces and viscous friction prevail over inertial values.

The transverse velocity component begins to influence on the flow, when amplitudes of pulsations $A > 2/3$. Pulsations in the entrance hydrodynamic length along the whole section occur with the first harmonic of the pulsation frequency of

the average velocity over the cross section when amplitudes of pulsations $A < 2/3$.

The stabilization length of the amplitude and pulsation phase of the velocity decrease with an increasing of the dimensionless frequency, moreover, this section has the longest length on the channel axis.

It was found that the length of hydrodynamic stabilization varies with the time and depends on the frequency and amplitude of pulsations. Its value, determined by the time-averaged velocity, is equal to the length for a steady flow. However, the maximum length of the entrance hydrodynamic length during the pulsation period increases with increasing of the amplitude of pulsations and decreases with increasing the frequency.

ACKNOWLEDGMENT

The scientific research was carried out at the cost of the grant from Russian Science Foundation (project No. 18-79-00281).

REFERENCES

- [1] Kovalenko L.V., Oshchepkov M.S., Mylnikova A.N., et al., 2018, "Specific structural features of microfluidic devices and their application", *Butlerov Communications*, 55(9) pp. 91–105.
- [2] Kindeeva O.V., Sorokin A.E., Haustov A.I., 2018, "Determination the physical parameters of culture medium in elements of the microfluidic biotechnical system" *Biotechnosphere*, 1, pp. 44–49.
- [3] He X., Ku D.N., 1994, "Unsteady entrance flow development in a straight tube" *J. Biomech. Eng.*, 16(3), pp. 355–361.
- [4] Schlichting H. *Grenzschicht-Theorie* // 1965. Karlsruhe, C. Braun.
- [5] Shiller L., 1922, "Die Entwicklung der laminaren Geschwindigkeitsverteilung und ihre Bedeutung für Zähigkeitsmessungen", *J. of Appl. Math. and Mech.*, 2(2), pp. 96–106.
- [6] Boboia J.R., Osterle J.F., 1961, "Finite difference analysis of plane Poiseuille and Couette flow developments" *Appl. Sci. Res.*, 10, Sec. A, pp. 265–276.
- [7] Valueva E.P., Purdin M.S., 2015, "The pulsating laminar flow in a rectangular channel" *Thermophys. Aeromech.*, 22(6), pp. 733–744.
- [8] Rouleau W. T., Osterle J.F., 1955, "The Application of Finite Difference Methods to Boundary-Layer Type Flows" *J. of the Aeronaut. Sci.* 22(4), pp. 249–254.
- [9] Purdin M.S., 2018, Program for the study of hydrodynamics with a developing pulsating laminar flow in a flat channel // Certificate of state registration of computer program No. 2018618169, October 7.
- [10] Terg S.M., 1951, "Basic problems of the theory of laminar flows", Moscow, Gostekhizdat.
- [11] Sparrow E.M., Lin S.H., Lundgren T.S., 1964, "Flow

Development in the hydrodynamic Entrance Region of Tubes and Ducts”, *Phys. Fluids.*, 7(3), pp. 338 – 347.

- [12] Liu J., 1974, “Flow of a Bingham Fluid in the Entrance Region of an Annular Tube”, M.S. Thesis. University of Wisconsin-Milwaukee.
- [13] Petukhov B.S., 1967, “Heat Exchange and Drag at a Laminar Fluid Flow in Pipes”, Moscow. *Energiya*. 412 p.
- [14] Valueva E.P., Purdin M.S., 2015, Program for calculating the laminar pulsating flow of incompressible fluid “Pulsating laminar flow” // Certificate of state registration of computer program No. 2015619049, August 24.
- [15] Valueva E.P., Purdin M.S., 2015, “Hydrodynamics and heat transfer for pulsating laminar flow in channels” *Therm. Eng.*, 9, pp. 636–644.
- [16] Valueva E.P., Purdin M.S., 2015, “Friction on the wall of a pulsating laminar flow in a flat and round channel”, Collection theses “Electronics, Electrical engineering and Energy”, Moscow, 3, pp. 127.